Journal of Electroanalytical Chemistry 922 (2022) 116710

Contents lists available at ScienceDirect

Journal of Electroanalytical Chemistry

journal homepage: www.elsevier.com/locate/jelechem

Passive direct methanol fuel cells acting as fully autonomous electrochemical biosensors: Application to sarcosine detection

Nádia S. Ferreira [a,b,c,d,1], Liliana P.T. Carneiro [a,b,c,d,1], Christian Viezzer [a], Maria J.T. Almeida [a], Ana C. Marques [d], Alexandra M.F.R. Pinto [d], Elvira Fortunato [d], M. Goreti F. Sales [a,b,c,*]

[a] BioMark@ISEP/CEB-LABBELS, School of Engineering, Polytechnic Institute of Porto, Porto, Portugal
[b] BioMark@UC/CEB-LABBELS, Department of Chemical Engineering, Faculty of Sciences and Technology, University of Coimbra, Portugal
[c] CEFT, Department of Chemical Engineering, Faculty of Engineering, University of Porto, Portugal
[d] CENIMAT i3N, Department of Materials Science, School of Science and Technology, NOVA University Lisbon and CEMOP/UNINOVA, Caparica, Portugal

ARTICLE INFO

Keywords:
Passive direct methanol fuel cell
Molecularly imprinted polymer
Electrochromic cell
Colour display
Sarcosine
Cancer biomarker

ABSTRACT

This work describes an innovative electrochemical biosensor that advances its autonomy toward an equipment-free design. The biosensor is powered by a passive direct methanol fuel cell (DMFC) and signals the response via an electrochromic display. Briefly, the anode side of the DMFC power source was modified with a biosensor layer developed using molecularly imprinted polymer (MIP) technology to detect sarcosine (an amino acid derivative that is a potential cancer biomarker). The biosensor layer was anchored on the surface of the anode carbon electrode (carbon black with Pt/Ru, 40:20). This was done by bulk radical polymerization with acrylamide, bis-acrylamide, and vinyl phosphonic acid. This layer selectively interacted with sarcosine when integrated into the passive DMFC (single or multiple, in a stack of 4), which acted as a transducer element in a concentration-dependent process. Serial assembly of a stack of hybrid DMFC/biosensor devices triggered an external electrochromic cell (EC) that produced a colour change. Calibrations showed a concentration-dependent sarcosine response from 3.2 to 2000 μM, which is compatible with the concentration of sarcosine in the blood of prostate cancer patients. The final DMFC/biosensor-EC platform showed a colour change perceptible to the naked eye in the presence of increasing sarcosine concentrations. This colour change was controlled by the DMFC operation, making this approach a self-controlled and self-signalling device.

Overall, this approach is a proof-of-concept for a fully autonomous biosensor powered by a chemical fuel. This simple and low-cost approach offers the potential to be deployed anywhere and is particularly suitable for point-of-care (POC) analysis.

1. Introduction

Electrochemical biosensors provide analytical data by combining a biorecognition unit with an electrochemical transduction element [1,2]. They are among the most popular biosensors because they are low cost, offer fast response,are potentially portable, and can be miniaturised - all attractive features for point-of-care (PoC) applications [3,4]. Despite all these advantages, the direct application of biosensors remains challenging for many reasons. One of them is their lack of autonomy [5,6].

This lack of self-sufficiency has been addressed in the past by the development of several approaches to self-powered biosensors described in the literature, including biosensors powered by dye-sensitised solar cells [7–10], and microbial/enzymatic fuel cells [11–14]. Despite the advantages of these transduction methods, there are still limitations in their application. Dye-sensitized solar cells cannot be operated at night and their performance is still low. Microbial and enzymatic fuel cells are very delicate systems that require more care in handling, and the performance to date is so low that this hinders their application, even for a small device.

Another approach for self-powered biosensors is the use of direct methanol fuel cells (DMFCs). DMFCs are electrochemical devices that generate electricity from methanol fuel and oxygen with high effi-

* Corresponding authors at: BioMark@UC, Department of Chemical Engineering, Faculty of Sciences and Technology of Coimbra University, Rua Sílvio Lima, Polo II, 3030-790 Coimbra, Portugal.
E-mail address: goreti.sales@eq.uc.pt (M. Goreti F. Sales).
[1] Equal participation as first authors.

https://doi.org/10.1016/j.jelechem.2022.116710
Received 5 May 2022; Received in revised form 31 July 2022; Accepted 13 August 2022
Available online 27 August 2022

ciency and vestigial emissions [15–17], which can be used for portable applications [15,18,19]. The first approach consisted of a heavy/large cell operated with flowing methanol solutions [20]. This operation under flow conditions provides good electrochemical performance of the fuel cell but hinders its application in PoC. Therefore, this design was recently developed into a cell that operates under steady-state conditions. It was designed in a previous report [21] and optimized to operate in passive mode, requiring only a few mL of a methanol solution. Although it had a lower electrochemical output, it provided enough energy to evaluate the effect of a target analyte, a cancer biomarker [22]. In this configuration, the biosensor was placed as an external element of the cell to reduce its impact on fuel cell performance.

Therefore, the work developed here is an innovative approach to the latest configuration in which the biosensor layer is integrated into the stationary DMFC [23]. This biosensor was directly attached to the surface of the anode catalyst that is commonly used in this type of Fuel Cell [24], and contains a molecularly imprinted polymer (MIP) as a sensing element for a target compound. This polymer was tailored by radical polymerization with suitable vinyl monomers (acrylamide, bis-acrylamidevinyl phosphonichonic acid) and radical initiators [25,26]. Upon removal of sarcosine, a potential cancer biomarker, from the polymeric network, binding sites are formed. As expected, these sites have a complementary shape to the imprinted molecule and allow complementary electrostatic interactions [27]. Since this MIP layer was located on the carbon-based anode electrode, which contained carbon fabric and Pt/Ru as metal catalysts, the sarcosine bond prevented the methanol from accessing the catalysts and thus hindered the fuel cell performance. This makes the operation of the DMFC concentration-dependent, leading to a new integrated DMFC biosensor device.

The autonomy of this platform also requires the elimination of all electronic components, since they require additional energy, and the electrochemical readings are usually collected by potentiostats. This limitation of autonomy has been solved in the past by coupling an electrochromic cell to the external circuit of the platform [8,9]. This cell has a colour that depends on the energy that passes through it. Since the energy arriving from the hybrid DMFC/biosensor depends on the concentration of sarcosine, the observed colour is concentration dependent. The electrochromic cell (EC) used in these works was organic and was made from PEDOT. However, we aimed at a more stable system for which we used an EC of inorganic nature prepared from tungstate, as tungsten oxide nanoparticles, as previously reported [28]. Since the inorganic ECs require more energy to show a colour change, the DMFC/biosensor cells were arranged in a 4-stack configuration.

As a proof-of-concept, this stand-alone biosensor was used to detect sarcosine, which has been reported in the literature as a potential biomarker for early detection of prostate cancer [29–31]. Sarcosine can be measured in urine and serum and can be used to study the progression of prostate cancer, as it is absent or present in negligible concentrations in healthy individuals [29]. Several approaches for screening sarcosine have been described in the literature (Table 1), including enzymatic assays [32–35], and molecular imprinted polymers (MIPs) [36–38]. None of these approaches offers the possibility of complete autonomy when used at the PoC.

Thus, this is the first work reporting on a DMFC/biosensor hybrid in a 4-stack configuration and in conjunction with an EC for visual transmission. This approach has been optimized under various conditions, with particular attention to the composition of the MIP layer, which is a novel material that has not been described before. The setup was characterized for analytical performance against sarcosine using two different media (buffer and synthetic serum). Operation of the system was tested with a single passive DMFC connected to a potentiostat and a 4-stack DMFC using the EC.

2. Experimental section

2.1. Reagents and solutions

All chemicals were of analytical grade and the water was ultrapure Milli-Q laboratory water. Measurements were performed in a buffer consisting of 2-morpholinoethanesulfonic acid (MES, AppliChem), 10 mM, pH 6.0. Sarcosine (Acros Organics) was used as the target compound, and standard solutions were prepared in MES buffer. For polymerization, 0.1 mM acrylamide (Acr − 99 %, Sigma Aldrich) and 0.5 mM bis-acrylamide (Bis-Acr − 99 %, Sigma Aldrich) in MES buffer were used, including 0.1 mM vinyl phosphonic acid (VPA − 97 %, Sigma-Aldrich) as a negatively charged monomer. Ammonium persulfate (APS, VWR Chemicals) and tetramethylethylenediamine (TEMED - from TCI) were used as initiators at a concentration of 1 % of the total concentration of monomers. For selectivity studies, foetal bovine serum (FBS) from Gibco was used at a 1000-fold dilution.

Carbon Black (CB) with PtRu (CB /PtRu, 40:20 wt%) catalyst (from Vulcan XC −72R, Quintech) was used as polymerization support. Liquid Nafion® (20 wt% in alcohols, Quintech) and 2-propanol (99.8 %, Panreac) were used for ink preparation. Solutions of 2.0 and 0.5 M methanol (Merck, HPLC grade) were used in the activation and calibration phases, respectively. Untreated plain carbon cloth (FuelCellsEtc) was used to apply the modified biosensor material (the anode of DMFC) and Pt carbon cloth (10 wt% Pt on Vulcan XC −72R, 1 mgPt/cm^2, Nafion coated, Quintech) was used as the cathode.

The EC material was prepared as WO_3 nanoparticles obtained with 0.15 M sodium tungstate dihydrate (99 %, ACROS Organics) and 3.0 M hydrochloric acid (37 %, Fluka). The resulting nanoparticles were dispersed in a 1:1 mixture of distilled water/ethylene glycol butyl ether. The electrolyte for the EC was a solution containing 1.0 M lithium perchlorate) and propylene carbonate (PC).

2.2. Fuel cell units

The passive DMFC devices were developed following [21] and are shown in Fig. 1. The single cell configuration includes the anode side (Fig. 1A) with a container to feed the methanol solution and the cathode side (Fig. 1B) with an “open” grid region to allow reaction with atmospheric oxygen. These electrodes were part of a membrane electrode assembly (MEA) containing the MIP-modified anode and a commercial cathode (Pt carbon mesh), separated by a solid Nafion® 115 membrane. The active area of this MEA was 2.25 cm^2. The DMFC also contained two metal plates that acted as current collectors and a rubber plate to insulate the system and prevent an electrical short. The 4-stack fuel cell configuration was achieved by connecting four DMFCs in series (Fig. 1C).

Both passive systems use natural capillary forces, diffusion and convection for their operation, without the additional power consumption and without additional components such as pumps to feed the reactants. These features and advantages of this type of systems make them suitable for portable applications, as they can be manufactured in a small and compact structure.

2.3. Biosensor element synthesis

The CB containing PtRu (40:20 wt%) catalyst (1 mg/mL) was suspended in MES buffer (pH ~ 6.0) by sonicating the mixture for 15 min. The target molecule (0.1 mM), sarcosine, and the negatively charged monomer (vinyl phosphonic acid) were previously incubated together for 1 h at 30 °C, then added to the previous mixture of CB and MES and incubated for 1 h at 30 °C with agitation. The polymerization mixture

Table 1
Literature review of Sarcosine biosensors with electrochemical detection.

Type	Detection	Support	Bioreceptor element	Autonomy	Linear response	LOD	Reference
Enzymatic	Electrochemical	Gold electrode	Sarcosine oxidase	No	0.1 – 100 μM	0.01 μM	[33]
Enzymatic	Electrochemical	Gold electrode	Sarcosine oxidase	No	0.1 – 100 μM	0.10 pM	[32]
Enzymatic	Electrochemical	Pt/MNP	Sarcosine oxidase	No	5–40 μM	0.24 μM	[46]
Enzymatic	Electrochemical	OECTs	Sarcosine oxidase	No	50 nM − 100 μM	50.0 nM	[47]
Enzymatic	Photoelectrochemical	ITO/NiO/PbS/Au electrode	Sarcosine oxidase	Yes	50 nM – 0.05 M	17.0 nM	[48]
Enzymatic	Electrochemical	CSPE	Sarcosine oxidase	No	10 – 400 μM	0.66 μM	[35]
MIP	Electrochemical	AuSPE	Electropolymerization of p-ATP	No	0.12 – 1.2 μM	8.50 nM	[36]
MIP	Electrochemical	Au electrode	MOFs	No	1–100 pM	0.40 pM	[37]
MIP	Electrochemical	Hydro-MeC-M	Electropolymerization of MAA	No	0.56– 22.5 μM	0.11 μM	[38]
MIP	Electrochemical	CB/PtRu	Acr/Bis-Acr/VPA	Yes	3.2–2000 μM	0.04 μM	**This work**

Pt/MNP: platinum loaded mesoporous nickel phosphonate; OECTs: Organic electrochemical transistors; CSPE: Carbon Screen Printed Electrode; AuSPE: Gold Screen-Printed Electrode; p-ATP: poly-aminothiophenol; MAA: Methacrylamide MOFs: metal–organic frameworks; Hydro-MeC-M: metal-coded hydrogel magnetic; CB/PtRu: Carbon Black/Platinum Ruthenium; Acr/Bis-Acr/VPA: Acrylamide/Bis-Acrylamide/Vinylphosphonic Acid.

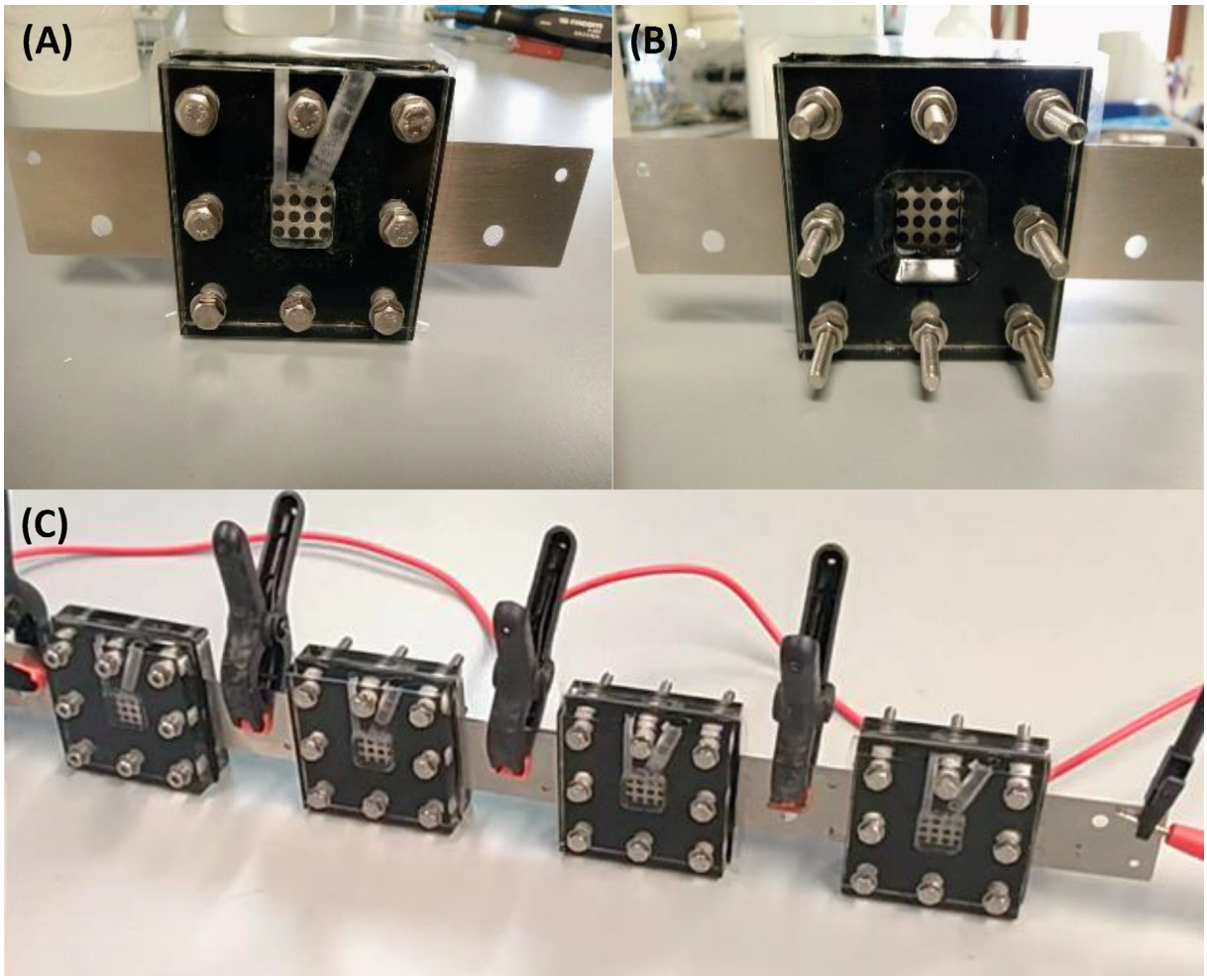

Fig. 1. Pictures of the passive DMFC device: (A) anode side of the fuel cell, containing a reservoir for introducing the methanol solution into the system; (B) cathode side of the fuel cell, with a grid opened to the atmosphere to allow the O_2 present in the atmospheric air to reach the electrode; (C) cell stack with the devices placed in series.

was then added to the flask. To initiate polymerization, both APS and TEMED were added to this suspension and stirred at 30 °C for 1 h. After the polymerization time, the mixture was centrifuged (so that the sensor material settled) and the supernatant was removed. The solid was washed by stirring in 0.5 M H_2SO_4 for 30 min to remove the template protein. To remove and neutralize residual monomers/proteins, the sensor material was washed with Milli-Q water (4 ×) and ethanol (1 ×) and dried overnight at 60 °C.

A control non-imprinted polymer (NIP) was also synthesised under the same conditions as the biosensor material, but without the template protein.

Special care was taken in the addition of the polymer layer around the catalytic particles because of its effect on the electrochemical activity of methanol. The polymer obtained should be permeable enough to allow some of the methanol to reach the catalytic particles, thus maintaining the operation of the fuel cell and the function of the biosensor.

2.4. Ink and electrode preparation

The MIP-CB-Pt/Ru nanoparticles were cast onto a carbon cloth support by incorporating them into a suitable ink formulation, spraying and drying. The ink suspension consisted of the biosensor material, 20 wt% Nafion® in alcohols (relative to the biosensor material), and 2-propanol. To apply the material with an airbrush, the solid should only make up to 10 % of the suspension to avoid clogging. The obtained suspension was sonicated for 30 min and applied to the support.

The application of the ink to the gas diffusion layer (GDL) of the fuel cell - the carbon cloth - was done by heating the carbon cloth to 60 °C (on a hot plate), applying the material to it with an airbrush, and letting it dry. The mass of the catalyst on the carbon cloth was controlled by weighing the support before and after deposition.

2.5. Electrochromic cell (EC)

The electrochromic device was produced according to Marques, et al. [28] with minor modifications. Briefly, the device was designed in image processing software (Adobe Illustrator, Adobe Systems Software, San Jose, CA, USA) with a planar 2-electrode configuration defined as working and counter electrodes (WE and CE, respectively). To pattern these electrodes and the electrical tracks, a CO_2 laser device with a wavelength of 10.6 μm (VLS3.50, Universal Laser Systems, Scottsdale, AZ, USA) was used to selectively remove the ITO layer from a PET/ITO foil with a sheet resistance of 30 Ω/square (Kintech Company, Shenzhen, China) with 10 W laser power at a scan rate of 1.27 m/s. Silver ink (Conductive compounds, Inc., New Hampshire, USA) was applied to the electrical tracks, followed by a curing process at 120 °C for 20 min, for ink's solvent evaporation. Then, 3 μL of 0.04 g/L WO_3 nanoparticles dispersed in water: ethylene glycol butyl ether were drop casted onto the WE and allowed to dry at 50 °C for 20 min. The WO_3 nanoparticles were prepared using an oven-assisted hydrothermal method according to Santos, et al [39] and Marques, et al. [28]. Finally, the EC device was encapsulated using a home-version laminator with a hydrophilic Whatman paper grade 4 (GE Healthcare, Chicago, IL, USA) placed on top of the WE/CE electrodes to obtain a simple configuration for easy integration into the DMFC/biosensor. A lithium-based electrolyte ($LiClO_4$: PC 1 M) was used in the EC.

The EC was integrated into an external circuit connected to the 4-stack DMFCs. At the time of use, the electrolyte was dropped onto the paper pad to first perform a control test (blank). In this case, the unit EC renders a blue colour at ≥1.5 V when fuel is added to the fuel cells. To test this unit, MeOH was removed from the container and replaced with the buffer solution, which was incubated there for 30 min. This solution was then removed and replaced again with methanol to check the electrical properties of the system. Then the MeOH solution was removed, and the container was filled with the less concentrated sarcosine standard solution; this solution was incubated for 30 min, then removed and replaced with MeOH to recheck the electrical properties and operation of EC. Then a bleaching process of the device was performed, followed by the test with the sarcosine sample. With increasing sarcosine incubation concentration, the fuel cell was unable to generate 1.5 V and the EC device could not achieve a coloured state.

2.6. Apparatus and fuel cell assembly

Electrochemical measurements were performed using a Metrohm Autolab Potentiostat/Galvanostat and a PGSTAT302N equipped with an FRA module and controlled by Nova software (NOVA 2.1). The cells were monitored at room temperature and atmospheric pressure. The anode was fed with 2.0 or 0.5 M MeOH solution (depending on whether it was used during activation or calibration) deposited on the reservoir, and the cathode used the O_2 of air.

The DMFC/biosensor assemblies are shown in Fig. 2. The biosensor element was first developed by free radical polymerization (Fig. 2A) and then placed on the anode side of the 4-stack DMFCs (Fig. 2B-C). These 4-stack/ DMFCs integrate the electrochemical cell (EC), which is electrically connected to simulate a single device without connecting a potentiostat. The generated energy powers the EC and promotes colour change according to the concentration of the biomarker present.

Generally, the polymer layer at the anode slows MeOH penetration, which limits its access to the Pt/Ru nanoparticles that are entrapped within the polymeric network, thereby influencing the rate of the electrochemical process generating current. This outcome is even more intense when proteins block the MeOH path towards the Pt/Ru catalyst by entering the imprinted cavity. This is schematically represented in Figure S1.

2.7. Electrochemical assays

For DMFC measurements, the cell was used at room temperature and atmospheric pressure. To evaluate the response of the DMFC with the modified imprinted anode, electrochemical measurements were performed using Sampled DC. This technique can be used to generate polarization curves, which are typically used for characterization when studying DMFCs. This involves entering a series of potentials and recording the corresponding current values. All measurements obtained were normalized to the catalyst mass (Pt/Ru) on the surface of the carbon cloth. The polarization curves of the DMFC and the DMFC/biosensor were normalized to obtain the maximum output of the system.

The fuel cell was previously activated by recording the polarization curves with 2.0 M MeOH solution until the power of the cell reached a stable value. Then, the fuel cell was left in Milli-Q water overnight to remove the excess MeOH on the electrode surface.

Calibration curves in buffered media were established by Sampled DC in sarcosine standard solutions (3.2, 16.0, 80.0, 400, 2000 μM) prepared in MES buffer. During calibration, each solution was incubated on the sensor surface (in the fuel cell anode reservoir) for 30 min, starting with the lowest concentration. After each incubation period, the sensor surface was washed with MES buffer; electrochemical measurements were performed with 0.5 M methanol. Selectivity studies were performed by calibrations in 1000-fold diluted FBS and spiked sarcosine standard solutions to evaluate the influence of serum on electrochemical readings.

3. Results and discussion

3.1. Operation of the passive fuel cell device and optimization

The performance of the passive DMFCs systems was evaluated prior to MIP assembly to identify the most suitable conditions. For this purpose, several polarization curves were measured with two different MeOH concentrations of 0.5 and 2.0 M, respectively, until signal stabilization. The polarization curves monitored the variation of cell potential against current density.

Fig. 3A shows the typical polarization curves of the DMFCs used in this work compared to the results obtained with different concentrations of MeOH. As expected, both current and power density were strongly affected by the MeOH concentration. However, considering that this system will function as a biosensor and the overall influence of the MIP film on the fuel cell results from it hindering the access of methanol to the Pt/Ru catalyst, using too much MeOH would result in a less sensitive system (experimental data not shown). Since MeOH is a small molecule, it can easily diffuse through the catalyst surface at higher concentrations and consequently affect the sensitivity of the final sensor (it would become insensitive to low concentrations of CEA).

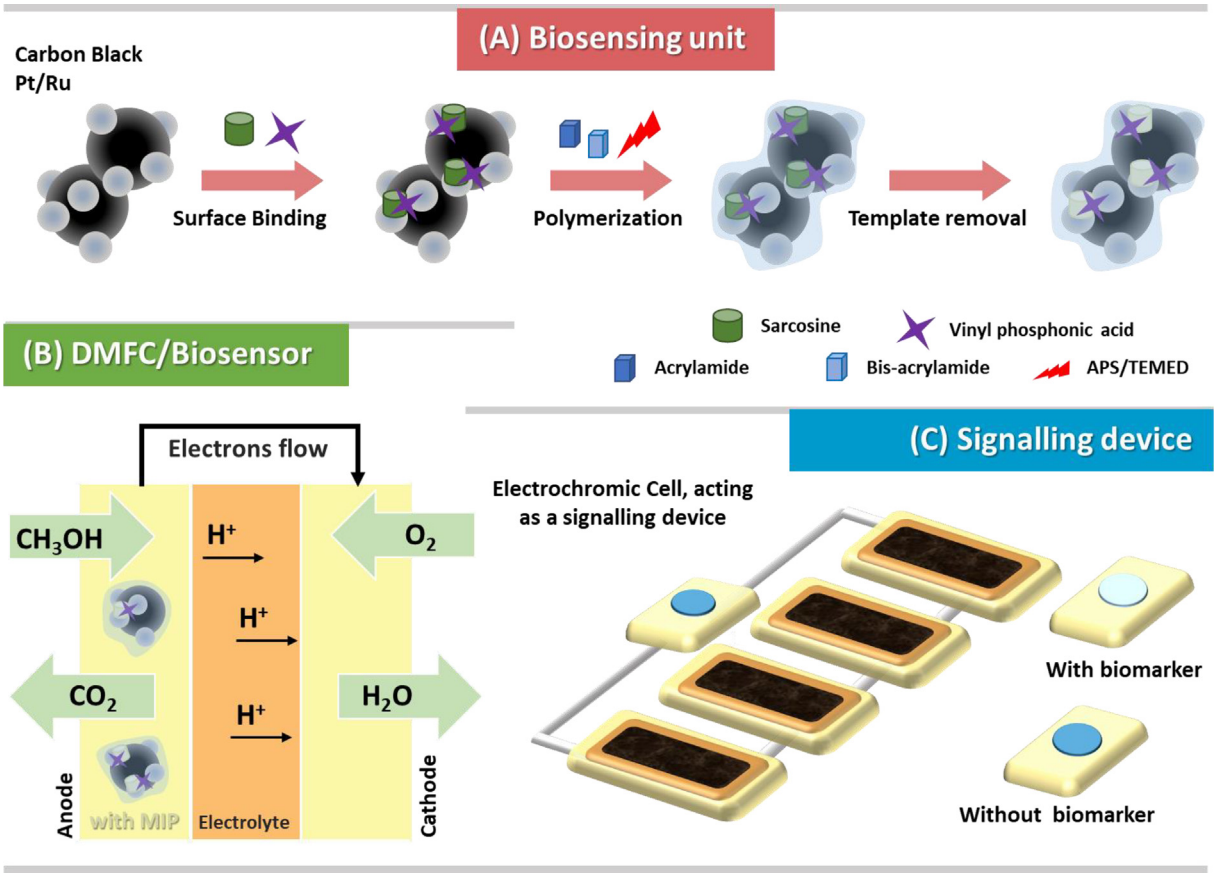

Fig. 2. Schematic representation of the various components of the final biosensor device, including (A) the synthesis of the MIP material around the CB-Pt/Ru; (B) the methanol fuel cell device and the membrane electrode unit (MEA); (C) and the 4-stack DMFC cells with biosensor, coupled with the signalling electrochromic cell.

With respect to the use of the DMFC with the MIP film as a biosensor, it is important that the signal is stable and that the power generated by the DMFC with the MIP can trigger the EC, which requires at least 1.5 V. Figure S2 shows that the DMFC with the sensing polymer on the anode operated with a 0.5 M MeOH solution and generates enough cell power to feed the EC when operated in stack mode. It was important to note that the system did not require a high MeOH concentration and the MeOH solution was only fed at specific times. The DMFC/biosensor device was very stable after consecutive incubations with MES buffer followed by feeding with a low MeOH concentration (Figure S2). This was also confirmed by calibrations with sarcosine solutions from independent cells.

3.2. Biosensing unit characterization

3.2.1. Spectroscopy analysis

To confirm the presence of the polymer on the surface of the carbon black catalyst (CB-Pt/Ru), the MIP films and the control materials (NIP) were analysed by FTIR-ATR spectroscopy (Fig. S3A) and Raman analysis (Fig. S3B).

Quite similar spectra were obtained in the analysis of FTIR-ATR (Fig. S3A), which was expected since these materials are mainly carbon-based, making it difficult to visualise the functional groups that might be present in the MIP/NIP samples [40]. However, the spectra of the polymerized MIP/NIP samples show significant differences compared to the unmodified CB-Pt/Ru. The observed differences are related to the vibrations of the functional groups of the monomers used in the polymerization and can be approximately assigned to the acrylate and amide groups (N—H, C—N, C=O) at 647 cm^{-1},750 cm^{-1}, 870 cm^{-1} and 1000–1100 cm^{-1} At 1260 cm^{-1}, a small band can be seen in the MIP/NIP samples, which can be associated with the P=O group of the vinylphosphonic acid, and at about 1400 cm^{-1}, a band with strong intensity appears in the modified polymer samples, which can be assigned to the carbonyl group insertion (C=O) [41]. The observed spectra differences are consistent and provide evidence for significant modification of the CB -Pt/Ru matrix support with the sensitive polymer.

Raman spectroscopy analysis (Fig. S3B) also proves the presence of the polymer on the surface of CB -Pt/Ru. All the samples examined showed the D and G peak of carbon. The D peak was located between 1200 and 1400 cm^{-1} and G peak between 1500 and 1600 cm^{-1}. The D peak is related to the disorder of the carbon structure (structural defects), while the G peak is related to the graphite present in the structure. In addition to these two peaks, one can observe other peaks between 100 and 800 cm^{-1} that probably indicate the presence of platinum [42] and ruthenium [43] in the samples. The ratio between the intensity of the D and G peaks was used to evaluate the carbon surface modifications [44]. The obtained I_D /I_G values can be found in the attached table in Fig. S3B. Analysis of these results shows that the ratio (I_D /I_G) of the MIP and NIP samples was significantly lower than that of the control sample, indicating that the presence of the polymer affects the Raman spectra of CB-Pt/Ru.

3.2.2. Calibrations in a single passive cell

Prior to calibration, the DMFC was activated with 2.0 M MeOH, as the use of a high concentration of MeOH allowed for rapid activation of the fuel cell. However, since the quantity of MeOH used to activate de fuel cell (2 M) was much higher than the one used for calibrations

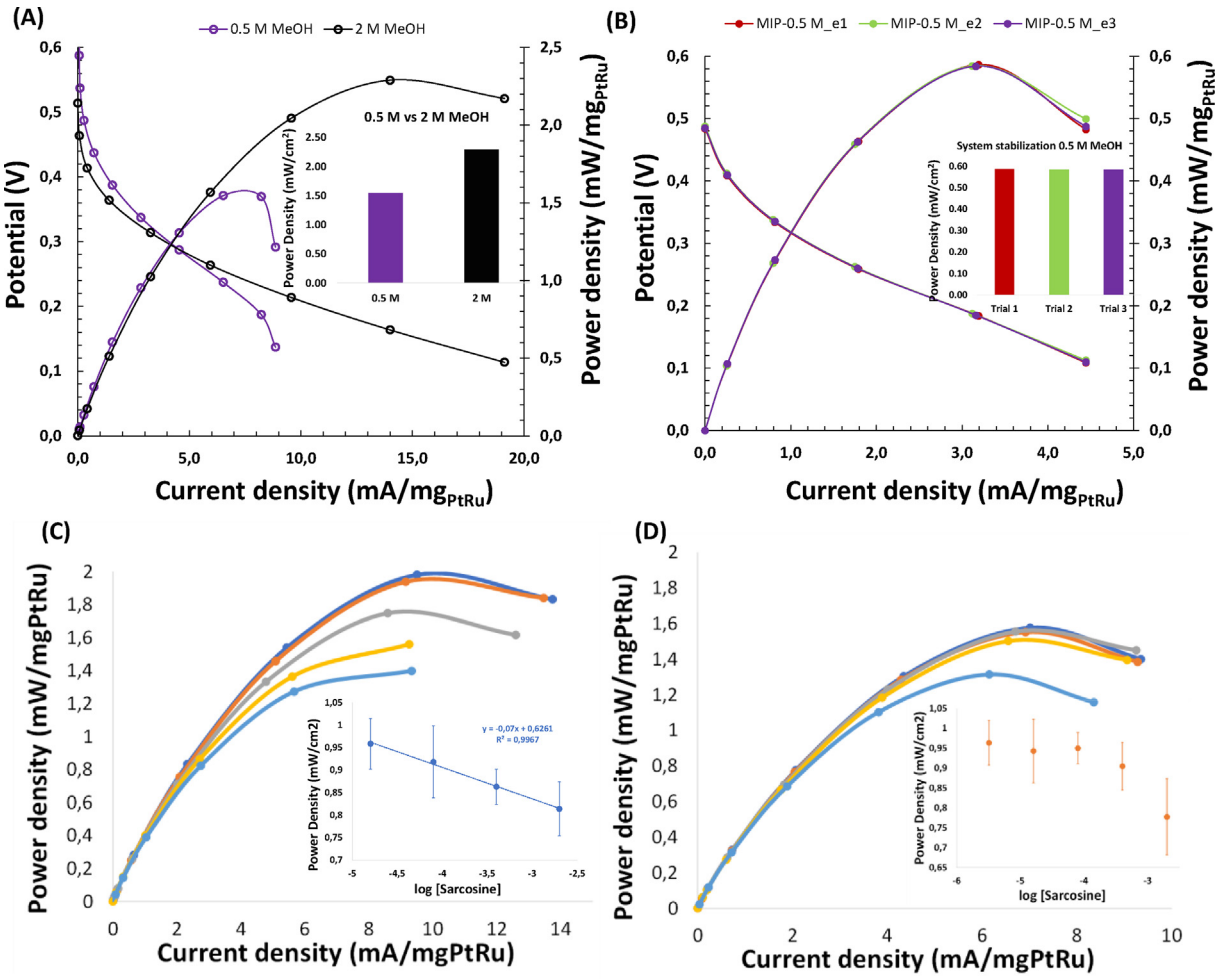

Fig. 3. Polarization curves of the passive DMFC device with (A) different MeOH concentrations (2 M and 0.5 M); stability of a DMFC with a printed anode using 0.5 M MeOH solution. The bar graphs are representative of the data obtained in both plots to better observe the stability of the system. Calibration data show (C) and (D) normalized calibration curve for the MIP shown compared to a control (NIP) obtained under the same conditions, and typical polarization curves of the DMFC biosensor device (MIP and NIP, respectively) for sarcosine with increasing concentrations ranging from 3.2 to 2000 μM in buffer.

(0.5 M), the greater part of MeOH adsorbed to the carbon cloth electrode had to be removed. This was made by leaving the fuel compartment of the activated cell with water. The single request here was that any remaining MeOH would be undetected when a solution of 0.5 M was placed on the fuel cell. This was achieved and granted, as may be seen in Figure S4.

3.2.2.1. Calibrations in buffer. Calibrations were always performed using sampled DC as electrochemical measurement and with sarcosine standard solutions prepared in MES buffer. Initially, only MES was incubated two to three times to check the influence of buffer solution on DMFC performance. This procedure was repeated until signal stability was achieved. The results obtained are shown in Fig. 3 and confirm the good stability of the system after several buffer incubations.

Each standard solution was incubated in the fuel cell for 30 min, after which the cell was washed with buffer. The performance of the cell was then measured using a 0.5 M MeOH solution at the anode compartment. The standard solutions incubated there had increasing sarcosine concentrations, namely 3.2, 16, 80, 400 and 2000 μM.

Fig. 3A shows the current and power densities obtained when calibrating a MIP, and Fig. 3B shows the calibration curve of the same MIP compared to the control (NIP). The MIP shows decreasing power with increasing sarcosine concentration and exhibits a logarithmic concentration-dependent behaviour from 3.2 to 2000 μM. This concentration interval mainly encompasses the sarcosine concentration in the blood of prostate cancer patients, which ranges from 2.0 to 10 μM, whereas the normal sarcosine level in healthy individuals is approximately 1.4 ± 0.6 μM. [33]. The NIP also showed decreasing performance like the MIP, but with lower intensity and only at higher concentrations. This different response of the MIP proves the binding of sarcosine to the imprinted binding sites and the subsequent blocking of the access of MeOH to the catalyst for its oxidation.

An additional control was performed to evaluate possible nonspecific adsorption of sarcosine on the carbon material. For this purpose, a calibration was performed using only the catalyst material (CB -Pt/Ru) under the same conditions as described previously. Fig. 4 shows the results of this control calibration. There is no significant change in the obtained performance after the incubation of sarcosine. These results show that the non-specific adsorption of sarcosine on the carbon surface is negligible. The limit of detection (LOD) was determined as described in [45], using linear regression method. In this case, LOD can be expressed as.

$$LOD = 3\left(\frac{Sa}{b}\right)$$

where, ***Sa*** means the standard deviation of the response of the curve, which can be obtained by the standard deviation of the regression line, and ***b*** is the slope of the calibration curve obtained from the equation of

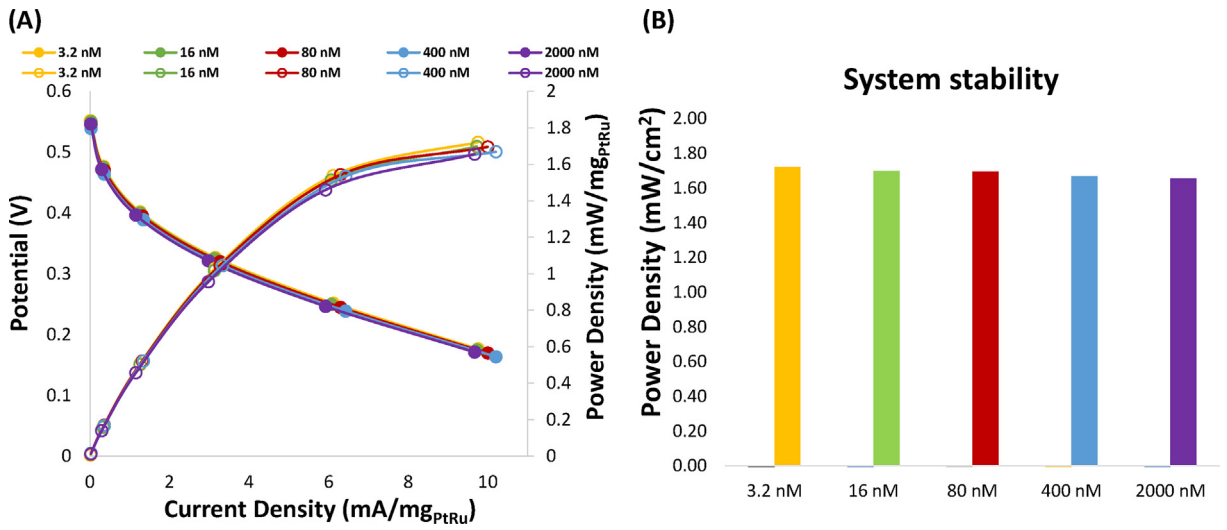

Fig. 4. Calibration data of the carbon support showing (A) typical polarization curves of the DMFC device with an unmodified anode (commercial) for sarcosine with increasing concentrations ranging from 3.2 to 2000 μM, in buffer, and (B) the normalized calibration curve obtained during calibration.

the calibration line. The calculation of LOD was performed using this equation, and the obtained LOD for this work was 0.04 μM.

3.2.2.2. Calibrations in serum. After optimization of the biosensor in the DMFC with standard solutions prepared in buffer, the selectivity of the biosensor was evaluated with standard solutions prepared in foetal bovine serum (FBS). FBS was used to mimic human samples and understand the effects of this fluid on the system. This FBS was diluted 1000-fold to reduce the presence of ions that could interfere with the Nafion® membrane in the DMFC.

The obtained results of a calibration in serum medium (Figure S5) show the changes in the performance of the cell with the increasing concentrations of sarcosine, with linearity from 3.2 to 2000 μM. The MIP reacts according to the previous calibrations with buffer (slope of 0.07, and correlation coefficient of 0.997), and the 1000-fold diluted serum has no significant interference in the cell, having a similar slope and correlation value of the calibration curve (slope of 0.0394, and correlation coefficient of 0.986). On the other hand, the NIP shows a random behaviour with a decrease in response when using the highest concentration of sarcosine, which could be the adsorption of the molecules present in the FBS. These results suggest that the biosensor is selective for sarcosine in the presence of FBS.

3.3. Final assembly DMFC-EC/Biosensor

The final DMFC-EC/biosensor combines the DMFC device, the biosensor unit, and the electrochromic cell, which operates as a unique and fully autonomous device. Following a previous work by some of the authors [28], where colour modulation at ±2 V was achieved, an optimization process was performed to reduce the electrical potential and power consumption of the device. For this purpose, the deposited volume of WO_3 nanoparticles in the WE was increased from 1.5 to 3 μL, achieving coloration at ±1.5 V and reducing the current density from 2.7 to 0.4 μA cm^{-2} (Figure S6). The hydrophilic paper encapsulated in the device, covering both WE and CE, served only to soak up the electrolyte during the time of use. Several hydrophilic papers were tested (data not shown). Due to its high porosity, the grade 4 Whatman paper proved capable of absorbing a large amount of electrolyte and allowing good contact with the nanoparticles, resulting in increased ionic charge.

Given the behaviour of the EC, the DMFC biosensor should generate enough current to power the electrochromic device, which in this case required a voltage of 1.5 V. To achieve this voltage, a stack of DMFCs had to be used, since each one generates only about 0.5 V. It is important to note the fine line between the initial cell potential and the potential reached after incubation of the target molecule. While there are potential differences that can be observed during calibration (with a potentiostat), the sarcosine molecule is small, and the potential variation is not so large that a cell stack with a very high initial potential can drop off so that it does not trigger the EC. This means that a cell stack with an initial potential as close as possible (slightly higher) to 1.5 V is necessary to obtain the desired colour change after incubation of the target molecule.

Originally, a stack of 5 DMFCs was to be used, but it turned out that a stack of 4 was sufficient to trigger the EC. Fig. 5A shows the EC in its initial state (white) and Fig. 5B-C shows the colour change of the EC, when interconnected with 4 and 5 cells, proving that a stack of 4 cells was sufficient to promote the colour change from white to blue. The colour change was fast and took about 20 s to reach full stability. It was also very stable and reproducible when different cells were compared. The colour reversal can also be easily achieved by simply switching the polarity, and two reversals can be performed while maintaining the effectiveness of the system.

After evaluating the electrical properties of EC, the stack of 4 DMFCs was incubated with MES buffer (during 30 min), as was done previously with the single DMFC. The influence of the buffer was small, as previously observed with the single cell, and the colour produced by EC was the same as that of the empty MeOH solution before buffer incubation. Then, the sarcosine standard solutions were incubated at the lowest concentration and the colour variation obtained is shown in Fig. 5D compared to the colour of the buffer. Analysis of the images shows that the colour produced by the buffer was intense. After incubation of the sarcosine standards, the colour loses intensity and almost disappears in the highest concentrated solution. Thus, as the sarcosine incubation concentration increased, the overall power of the 4-stack DMFC decreased and it was no longer able to generate 1.5 V, so the device EC did not receive any colour.

The EC in combination with the DMFC biosensor made it possible to obtain a self-powered and self-signalling system that does not require a potentiostat to enable quantification of the sarcosine target by a colour change in the gradient that is perceptible to the naked eye.

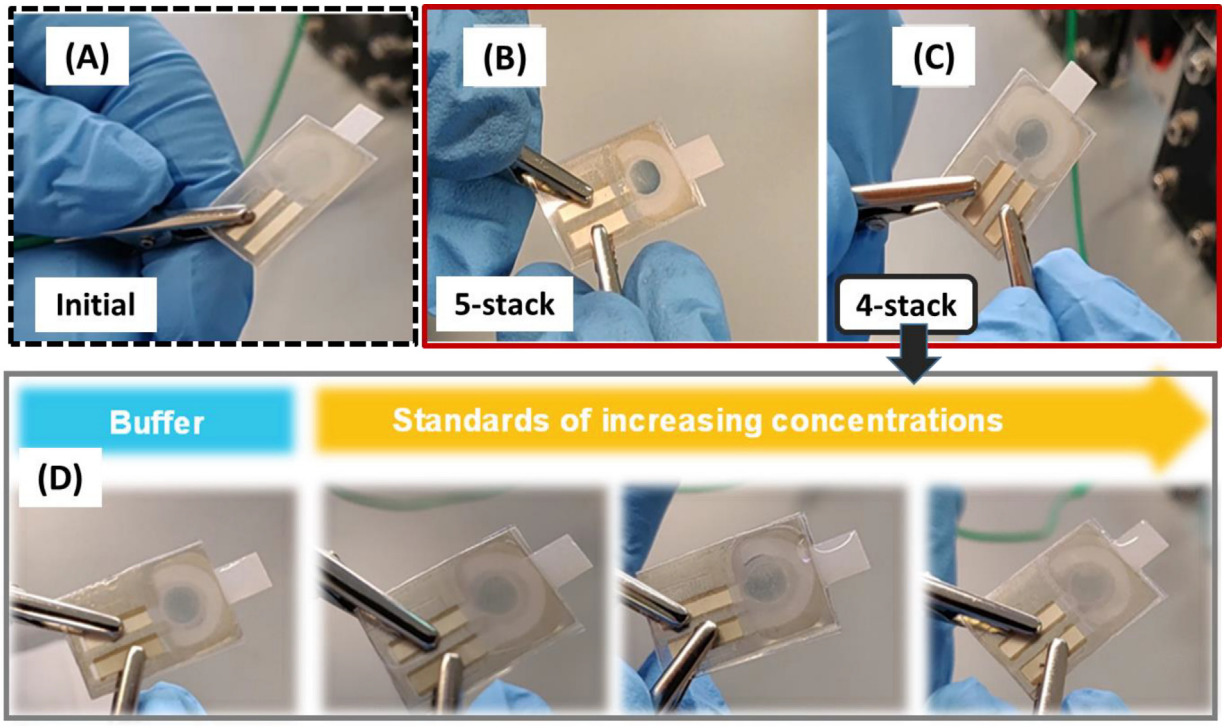

Fig. 5. Images of the electrochromic cell (EC) in operation: (A) in the initial state before coupling with the DMFC biosensor (white colour); (B) after coupling with a 5-stack DMFC; and (C) 4-stack DMFC that was able to trigger the EC from white to blue; (D) colour gradient obtained with a 4-stack DMFC biosensor from incubation in MES buffer (blank signal) to increasing sarcosine concentrations, showing the colour change from blue to very light blue.

4. Conclusion

Using a passive DMFC as a power supply, a MIP as a biosensor unit, and an EC as a signalling element, a self-powered and self-signalling biosensor was developed to determine sarcosine.

The self-powered approach was achieved by developing a MIP film on the catalyst material of the fuel cell operating under steady-state conditions. Calibrations in buffer and FBS confirmed the good selectivity and sensitivity of the combined device for sarcosine. The electrochemical performance of the DMFC-modified biosensor showed a linear trend with the log concentration of sarcosine ranging from 3.2 to 2000 μM in both buffer and FBS (compatible with the concentrations expected in real samples).

The self-signalling approach was achieved by coupling an EC to the DMFC-EC/biosensor. This EC showed an intense blue coloration at maximum cell power and this coloration decreased with decreasing power values. The DMFC-EC/biosensor showed a naked eye detectable colour change in the presence of sarcosine standards, proving that it is possible to obtain a self-sustaining and self-signalling system capable of detecting sarcosine within seconds.

Overall, this type of setup may prove to be a promising approach that has never been reported before to achieve sensitive analytical analysis using instrument-free methods. The final DMFC-EC/biosensor setup could be improved in a future work by miniaturising the four stack DMFCs and using another EC with lower potential requirement, allowing the use of a single DMFC.

CRediT authorship contribution statement

Nádia S. Ferreira: Investigation, Methodology, Data curation, Visualization, Validation, Writing – original draft. **Liliana P.T. Carneiro:** Investigation, Methodology, Data curation, Validation, Writing – original draft. **Christian Viezzer:** Investigation, Data curation. **Maria J.T. Almeida:** Investigation, Data curation. **Ana C. Marques:** Investigation, Visualization, Writing – review & editing. **Alexandra M.F.R. Pinto:** Conceptualization, Validation, Supervision, Resources, Writing – review & editing. **Elvira Fortunato:** Conceptualization, Funding acquisition, Project administration, Supervision, Resources, Writing – review & editing. **M. Goreti F. Sales:** Conceptualization, Funding acquisition, Project administration, Methodology, Validation, Supervision, Resources, Writing – review & editing.

Data availability

Data will be made available on request.

Declaration of Competing Interest

The authors declare that they have no known competing financial interests or personal relationships that could have appeared to influence the work reported in this paper.

Acknowledgements

The authors acknowledge the financial support of EU-Horizon 2020 (Symbiotic, FET-Open, GA665046), and from national funds from FCT - Fundação para a Ciência e a Tecnologia, I.P., in the scope of the projects LA/P/0037/2020, UIDP/50025/2020, UIDB/50025/2020 and UID/EMS/00532/2019. Nádia Ferreira (SFRH/BD/122955/2016), Liliana Carneiro (SFRH/BD/122954/2016), and Ana Carolina Marques (SFRH/BD/115173/2016) acknowledge Fundação para a Ciência e Tecnologia (FCT) for financial support.

Appendix A. Supplementary data

Supplementary data to this article can be found online at https://doi.org/10.1016/j.jelechem.2022.116710.

References

[1] P. Martinkova, A. Kostelnik, T. Valek, M. Pohanka, Main streams in the construction of biosensors and their applications, Int. J. Electrochem. Sci. 12 (2017) 7386–7403, https://doi.org/10.20964/2017.08.02.

[2] D.R. Thévenot, K. Toth, R.A. Durst, G.S. Wilson, Electrochemical biosensors: Recommended definitions and classification, Biosens. Bioelectron. 16 (2001) 121–131, https://doi.org/10.1016/S0956-5663(01)00115-4.

[3] W. Zhang, R. Wang, F. Luo, P. Wang, Z. Lin, Miniaturized electrochemical sensors and their point-of-care applications, Chinese Chem. Lett. 31 (2020) 589–600, https://doi.org/10.1016/j.cclet.2019.09.022.

[4] E.T.S.G. da Silva, D.E.P. Souto, J.T.C. Barragan, J. de F. Giarola, A.C.M. de Moraes, L.T. Kubota, Electrochemical biosensors in point-of-care devices: recent advances and future trends, ChemElectroChem. 4 (4) (2017) 778–794.

[5] Y.D. Han, H.J. Chun, H.C. Yoon, Low-cost point-of-care biosensors using common electronic components as transducers, Korean BioChip Soc. 14 (2020) 32–47, https://doi.org/10.1007/s13206-020-4104-8.

[6] D. Grieshaber, R. MacKenzie, J. Vörös, E. Reimhult, Electrochemical biosensors - sensor principles and architectures, Sensors. 8 (3) (2008) 1400–1458.

[7] L.A.A.N.A. Truta, F.T.C. Moreira, M.G.F. Sales, A dye-sensitized solar cell acting as the electrical reading box of an immunosensor: Application to CEA determination, Biosens. Bioelectron. 107 (2018) 94–102, https://doi.org/10.1016/j.bios.2018.02.011.

[8] A.P.M. Tavares, L.A.A.N.A. Truta, F.T.C. Moreira, L.P.T. Carneiro, M.G.F. Sales, Self-powered and self-signalled autonomous electrochemical biosensor applied to cancinoembryonic antigen determination, Biosens. Bioelectron. 140 (2019), https://doi.org/10.1016/j.bios.2019.111320 111320.

[9] A.P.M. Tavares, L.A.A.N.A. Truta, F.T.C. Moreira, G. Minas, M.G.F. Sales, Photovoltaics, plasmonics, plastic antibodies and electrochromism combined for a novel generation of self-powered and self-signalled electrochemical biomimetic sensors, Biosens. Bioelectron. 137 (2019) 72–81, https://doi.org/10.1016/j.bios.2019.04.055.

[10] F.T.C. Moreira, M.G.F. Sales, Autonomous biosensing device merged with photovoltaic technology for cancer biomarker detection, J. Electroanal. Chem. 855 (2019), https://doi.org/10.1016/j.jelechem.2019.113611 113611.

[11] S. Hao, X. Sun, H. Zhang, J. Zhai, S. Dong, Recent development of biofuel cell based self-powered biosensors, J. Mater. Chem. B. 8 (2020) 3393–3407, https://doi.org/10.1039/c9tb02428j.

[12] F.T.C. Moreira, M.G.F. Sale, M. Di, Towards timely Alzheimer diagnosis : A self-powered amperometric biosensor for the neurotransmitter acetylcholine, Biosens. Bioelectron. 87 (2017) 607–614, https://doi.org/10.1016/j.bios.2016.08.104.

[13] M. Kim, M. Sik, M. Gadd, H. Joo, A novel biomonitoring system using microbial fuel cells, J. Environ. Monit. 9 (2007) 1323–1328, https://doi.org/10.1039/b713114c.

[14] Y. Han, J.M. Chabu, S. Hu, L. Deng, Y. Liu, S. Guo, Rational tuning of the electrocatalytic nanobiointerface for a " turn-off " biofuel-cell-based self-powered biosensor for p53 protein, Chem. Eur. J. 21 (2015) 13045–13051, https://doi.org/10.1002/chem.201502062.

[15] M.S. Alias, S.K. Kamarudin, A.M. Zainoodin, M.S. Masdar, Active direct methanol fuel cell: An overview, Int. J. Hydrogen Energy. 45 (2020) 19620–19641, https://doi.org/10.1016/j.ijhydene.2020.04.202.

[16] Z.A.C. Ramli, S.K. Kamarudin, Platinum-based catalysts on various carbon supports and conducting polymers for direct methanol fuel cell applications: a review, Nanoscale Res. Lett. 13 (2018), https://doi.org/10.1186/s11671-018-2799-4.

[17] N.V. Raghvaiah, G.N. Srinivasulu, I.H. Prasad, Review of challenges in direct methanol fuel cell and contemporary status, Res. Appl. Therm. Eng. 3 (2020) 1–8, https://doi.org/10.5281/zenodo.3989515.

[18] N. Sazali, W.N. Wan Salleh, A.S. Jamaludin, M.N. Mhd Razali, New perspectives on fuel cell technology: A brief review, Membranes (Basel). 10 (5) (2020) 99.

[19] M. Goor, S. Menkin, E. Peled, High power direct methanol fuel cell for mobility and portable applications, Int. J. Hydrogen Energy. 44 (2018) 3138–3143, https://doi.org/10.1016/j.ijhydene.2018.12.019.

[20] M.G.F. Sales, L. Brandão, Autonomous electrochemical biosensors: A new vision to direct methanol fuel cells, Biosens. Bioelectron. 98 (2017) 428–436, https://doi.org/10.1016/j.bios.2017.07.021.

[21] B.A. Berns, M.F. Torres, V.B. Oliveira, Performance of passive Direct Methanol Fuel Cell : modelling and experimental studies, U.Porto J. Eng. 1 (2015) 89–103. https://journalengineering.fe.up.pt/article/view/110/111.

[22] L.P.T. Carneiro, N.S. Ferreira, A.P.M. Tavares, A.M.F.R. Pinto, A. Mendes, M.G.F. Sales, A passive direct methanol fuel cell as transducer of an electrochemical sensor, applied to the detection of carcinoembryonic antigen, Biosens. Bioelectron. 175 (2021) 1–9, https://doi.org/10.1016/j.bios.2020.112877.

[23] L.P.T. Carneiro, A.M.F.R. Pinto, A. Mendes, M. Goreti, An all-in-one approach for self-powered sensing: A methanol fuel cell modified with a molecularly imprinted polymer for cancer biomarker detection, J. Electroanal. Chem. 906 (2022), https://doi.org/10.1016/j.jelechem.2022.116009 116009.

[24] S. Khodabakhshi, P.F. Fulvio, E. Andreoli, Carbon black reborn: Structure and chemistry for renewable energy harnessing, Carbon N. Y. 162 (2020) 604–649, https://doi.org/10.1016/j.carbon.2020.02.058.

[25] M.F. Frasco, L.A.A.N.A. Truta, M.G.F. Sales, F.T.C. Moreira, Imprinting technology in electrochemical biomimetic sensors, Sensors 17 (2017) 523, https://doi.org/10.3390/s17030523.

[26] J.J. Belbruno, Molecularly imprinted polymers, Chem. Rev. 119 (2019) 94–119, https://doi.org/10.1021/acs.chemrev.8b00171.

[27] L. Chen, X. Wang, W. Lu, X. Wu, J. Li, Molecular imprinting: perspectives and applications, Chem. Soc. Rev. 45 (2016) 2137–2211, https://doi.org/10.1039/c6cs00061d.

[28] A. Marques, L. Santos, S. Pereira, U. Emanuele, S. Sinopoli, R. Igreja, G. Sales, R. Martins, E. Fortunato, A planar electrochromic device using WO3 nanoparticles and a modified paper-based electrolyte, Proceedings. 2 (2018) 1065, https://doi.org/10.3390/proceedings2131065.

[29] M. Ferro, C. Buonerba, D. Terracciano, G. Lucarelli, V. Cosimato, D. Bottero, V.M. Deliu, P. Ditonno, S. Perdonà, R. Autorino, I. Coman, S. De Placido, G. Di Lorenzo, O. De Cobelli, Biomarkers in localized prostate cancer, Futur. Oncol. 12 (2016) 399–411, https://doi.org/10.2217/fon.15.318.

[30] S. Koutros, T.E. Meyer, S.D. Fox, H.J. Issaq, T.D. Veenstra, W.Y. Huang, K. Yu, D. Albanes, L.W. Chu, G. Andriole, R.N. Hoover, A.W. Hsing, S.I. Berndt, Prospective evaluation of serum sarcosine and risk of prostate cancer in the prostate, lung, colorectal and ovarian cancer screening trial, Carcinogenesis. 34 (2013) 2281–2285, https://doi.org/10.1093/carcin/bgt176.

[31] A. Sreekumar, L.M. Poisson, T.M. Rajendiran, A.P. Khan, Q. Cao, J. Yu, B. Laxman, R. Mehra, R.J. Lonigro, Y. Li, M.K. Nyati, A. Ahsan, S. Kalyana-Sundaram, B. Han, X. Cao, J. Byun, G.S. Omenn, D. Ghosh, S. Pennathur, D.C. Alexander, A. Berger, J. R. Shuster, J.T. Wei, S. Varambally, C. Beecher, A.M. Chinnaiyan, Metabolomic profiles delineate potential role for sarcosine in prostate cancer progression, Nature. 457 (2009) 910–914, https://doi.org/10.1038/nature07762.

[32] V. Narwal, P. Kumar, P. Joon, C.S. Pundir, Fabrication of an amperometric sarcosine biosensor based on sarcosine oxidase/chitosan/CuNPs/c-MWCNT/Au electrode for detection of prostate cancer, Enzyme Microb. Technol. 113 (2018) 44–51, https://doi.org/10.1016/j.enzmictec.2018.02.010.

[33] P. Kumar, V. Narwal, R. Jaiwal, C.S. Pundir, Construction and application of amperometric sarcosine biosensor based on SOxNPs/AuE for determination of prostate cancer, Biosens. Bioelectron. 122 (2018) 140–146, https://doi.org/10.1016/j.bios.2018.09.003.

[34] C. Wang, Y. Wang, H. Zhang, H. Deng, X. Xiong, C. Li, W. Li, Molecularly imprinted photoelectrochemical sensor for carcinoembryonic antigen based on polymerized ionic liquid hydrogel and hollow gold nanoballs/MoSe2 nanosheets, Anal. Chim. Acta. 1090 (2019) 64–71, https://doi.org/10.1016/j.aca.2019.09.029.

[35] T. Rajarathinam, M. Kwon, D. Thirumalai, S. Kim, S. Lee, J.-H. Yoon, H.-J. Paik, S. Kim, J. Lee, H.K. Ha, S.-C. Chang, Polymer-dispersed reduced graphene oxide nanosheets and Prussian blue modified biosensor for amperometric detection of sarcosine, Anal. Chim. Acta. 1175 (2021) 338749.

[36] T.P. Nguy, T. Van Phi, D.T.N. Tram, K. Eersels, P. Wagner, T.T.N. Lien, Development of an impedimetric sensor for the label-free detection of the amino acid sarcosine with molecularly imprinted polymer receptors, Sensors Actuators, B Chem. 246 (2017) 461–470, https://doi.org/10.1016/j.snb.2017.02.101.

[37] P. Tang, Y. Wang, F. He, Electrochemical sensor based on super-magnetic metal–organic framework@molecularly imprinted polymer for Sarcosine detection in urine, J. Saudi Chem. Soc. 24 (2020) 620–630, https://doi.org/10.1016/j.jscs.2020.06.004.

[38] Z. Ramezani, M. Safdarian, A.A. Ghadiri, Metal-coded hydrogel magnetic molecularly imprinted polymer for preconcentration and cleanup of sarcosine: Determination in urine; coupled to on-column capillary electrophoresis, Talanta. 230 (2021), https://doi.org/10.1016/j.talanta.2021.122309 122309.

[39] L. Santos, J.P. Neto, A. Crespo, D. Nunes, N. Costa, I.M. Fonseca, P. Barquinha, L. Pereira, J. Silva, R. Martins, E. Fortunato, WO3 nanoparticle-based conformable pH sensor, ACS Appl. Mater. Interfaces. 6 (2014) 12226–12234, https://doi.org/10.1021/am501724h.

[40] M. Claybourn, P. Colombel, J. Chalmers, Characterization of carbon-filled polymers by specular reflectance, Appl. Spectrosc. 45 (1991) 279–286. https://doi.org/https://doi.org/10.1366/0003702914337669.

[41] J. Coates, Interpretation of infrared spectra, a practical approach, Encycl Anal. Chem. (2006) 10815–10837, https://doi.org/10.1002/9780470027318.a5606.

[42] Y.F. Huang, P.J. Kooyman, M.T.M. Koper, Intermediate stages of electrochemical oxidation of single-crystalline platinum revealed by in situ Raman spectroscopy, Nat. Commun. 7 (2016) 1–7, https://doi.org/10.1038/ncomms12440.

[43] Y. Hyun, J.Y. Choi, H.K. Park, C.S. Lee, Synthesis and electrochemical performance of ruthenium oxide-coated carbon nanofibers as anode materials for lithium secondary batteries, Appl. Surf. Sci. 388 (2016) 274–280, https://doi.org/10.1016/j.apsusc.2016.01.095.

[44] M.S. Dresselhaus, A. Jorio, R. Saito, Characterizing graphene, graphite, and carbon nanotubes by raman spectroscopy, Annu. Rev. Condens. Matter Phys. 1 (2010) 89–108, https://doi.org/10.1146/annurev-conmatphys-070909-103919.

[45] A. Shrivastava, V. Gupta, Methods for the determination of limit of detection and limit of quantitation of the analytical methods, Chronicles Young Sci. 2 (2011) 21, https://doi.org/10.4103/2229-5186.79345.

[46] Q. Wang, C. Yang, Q. Yang, S. Yu, H. Yang, Platinum-loaded mesoporous nickel phosphonate and its electrochemical application for sarcosine detection, Anal. Chim. Acta. 1046 (2019) 93–98, https://doi.org/10.1016/j.aca.2018.09.027.

[47] J. Hu, W. Wei, S. Ke, X. Zeng, P. Lin, A novel and sensitive sarcosine biosensor based on organic electrochemical transistor, Electrochim. Acta. 307 (2019) 100–106, https://doi.org/10.1016/j.electacta.2019.03.180.

[48] H. Wang, Y. Qi, D. Wu, Q. Wei, A photoelectrochemical self-powered sensor for the detection of sarcosine based on NiO NSs/PbS/Au NPs as photocathodic material, J. Hazard. Mater. 416 (2021), https://doi.org/10.1016/j.jhazmat.2021.126201 126201.